Journal of Catalysis 262 (2009) 9–17

Contents lists available at ScienceDirect

Journal of Catalysis

www.elsevier.com/locate/jcat

Synthesis of a new type of immobilized chiral salen Mn(III) complex as effective catalysts for asymmetric epoxidation of unfunctionalized olefins

Biwei Gong, Xiangkai Fu *, Junxian Chen, Yuedong Li, Xiaochuan Zou, Xiaobo Tu, Pingping Ding, Liping Ma

College of Chemistry and Chemical Engineering, Research Institute of Applied Chemistry Southwest University, The Key Laboratory of Applied Chemistry of Chongqing Municipality, Chongqing, 400715, China

ARTICLE INFO

Article history:
Received 29 July 2008
Revised 7 November 2008
Accepted 21 November 2008
Available online 7 January 2009

Keywords:
Zirconium poly(styrene-phenylvinylphosphonate)-phosphate
Chiral salen Mn(III)
Heterogeneous catalysts
Unfunctionalized olefins
Enantioselective epoxidation

ABSTRACT

A new type of inorganic–organic hybrid materials—zirconium poly(styrene-phenylvinylphosphonate)-phosphate (ZPS-PVPA) was designed and synthesized. A series of new heterogeneous catalysts was obtained by grafting diamine or polyamine on ZPS-PVPA and subsequently axial coordination with chiral salen Mn(III) complexes. All the synthesized heterogeneous catalysts exhibited great activity and enantioselectivity in the asymmetric epoxidation of unfunctionalized olefins. Especially, in the epoxidation of α-methylstyrene, both the conversion and enantiometric excess (ee) could exceed 99%. Furthermore, the catalysts were conveniently separated from the reaction system by simple precipitation in hexane and could be reused at least ten times without significant loss of activity and enantioselectivity.

1. Introduction

The epoxidation of unfunctional olefins is of great importance in synthesis of chiral epoxides, which are widely used in the manufacture of drugs, vitamins, fragrances and other optical materials. Chiral salen Mn(III) complexes [1,2] exhibit excellent catalytic activity and enantioselectivity for the homogeneous asymmetric epoxidation of various unfunctional olefins [3]. However, separation of such homogeneous catalysts from the reaction mixture and reuse are still problematic [4]. To address this issue, several groups have tried to overcome this difficulty by heterogenizing the homogeneous chiral salen Mn(III) complexes (e.g., immobilization of salen Mn(III) complex on mesoporous materials [5,6], activated carbon [7,8], zeolite Y [9], poly-system [10], clay compounds [11], and inorganic membranes [12]), thereby creating chiral heterogeneous catalyst that can be readily recovered from reaction mixtures. Unfortunately, despite their excellent performance in easy separation, the heterogeneous catalysts often suffer from decreased catalytic efficiency which likely due to the leaching of salen Mn(III) complexes during reaction and/or the inaccessibility of the reagents to the reactive centers [13]. Therefore, a new type and effective heterogeneous chiral salen Mn(III) catalysts is urgently needed for asymmetric epoxidation of various unfunctional olefins.

Zirconium phosphates and zirconium phosphonates are types of layered multi-functional materials with high thermal and chemical stability [14]. Current research in the zirconium phosphates and zirconium phosphonates field is active, which have involved mainly adsorbent [15–17], inorganic ion exchangers [18,19], intercalation chemistry [20,21], sensor and proton conductivity [22] and catalysts [23–25]. However, few of the mixed zirconium phosphate-phosphonates $Zr(HPO_4)_{2-x}(O_3PG)_x$ ($x = 0$–2, G is organic group) in which inorganic/organic molar ratio and organic group can be modulated for special purposes are reported, especially in the application of catalyst support for homogeneous salen Mn(III) catalyst in heterogeneous catalysis. For this purpose, we have reported the synthesis of oligostyrenyl phosphonous acid (OSPUA) [26] and corresponding zirconium oligostyrenyl-phosphonate-phosphate (ZSPP). As a new type of organic–inorganic hybrid material, ZSPP has been used to prepare a series of new solid acid catalysts with high thermal stability (over 200 °C) and reusability [27,28]. Recently, we have successfully introduced polyamines into chloromethyl-zirconium oligostyrenyl phosphonate hydrogen phosphate (ZCMSPP) and anchored polyamines molybdenum (VI) complexes [29], which performed high conversion, enantioselectivity and reusability. We have also reported the chiral salen Mn(III) complex axially immobilized on diamine modified ZSPP and their catalytic epoxidation of styrene [30], which showed high enantioselectivity and could be reused at least five times without significant loss of activity and enantioselectivity.

Based on our previous work [14,26–30], in the present study, linear styrene-phenylvinylphosphonic acid copolymer and its corresponding zirconium poly(styrene-phenylvinylphosphonate)-phosphate (ZPS-PVPA) were synthesized and diamine or polyamine

* Corresponding author. Fax: +86 23 68254000.
E-mail address: fxk@swu.edu.cn (X.K. Fu).

0021-9517/$ – see front matter
doi:10.1016/j.jcat.2008.11.027

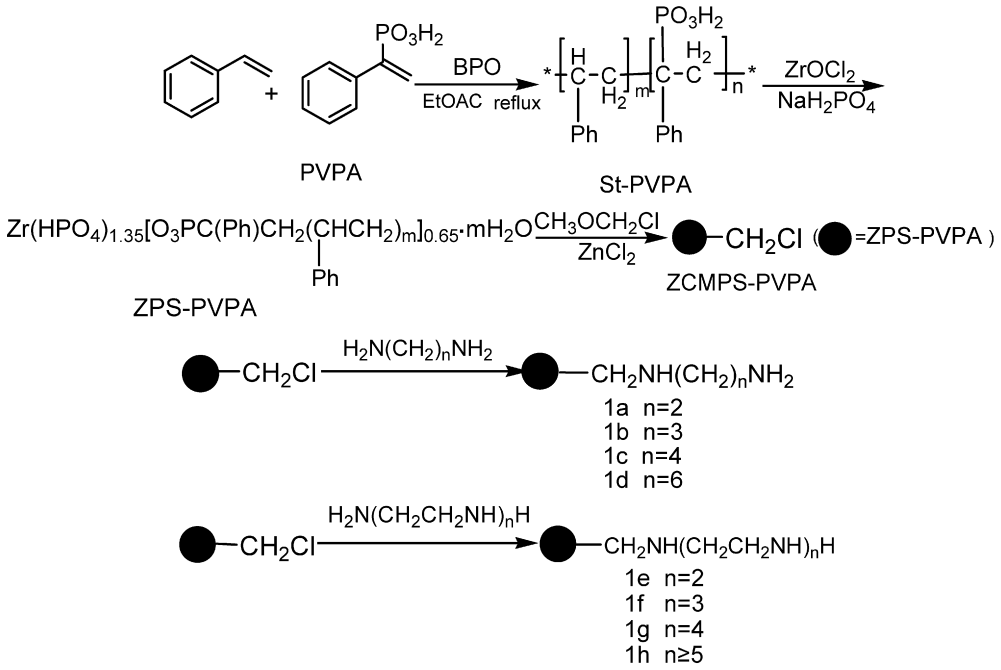

Scheme 1. Synthesis of the support.

modified ZPS-PVPA were used to immobilize the chiral salen Mn(III) complexes through axial coordination. The immobilized catalysts (3a–3h) effectively catalyzed epoxidation of styrene and α-methylstyrene (ee, 50 to 78% and 86 to >99%) with m-CPBA or NaClO. These results are significantly better than those achieved with the homogeneous catalyst 2 under the same reaction conditions (ee, 47% and 65%). Remarkably, the immobilized catalysts could be reused at least ten times without significant loss of activity and enantioselectivity.

2. Experiment

2.1. Materials and methods

(1R,2R)-(-)-1, 2-diaminocyclohexane, chloromethyl methyl ether (toxic compound), α-methylstyrene, *n*-nonane, 4-phenylpyridine *N*-oxide (PPNO), *N*-methylmorpholine *N*-oxide (NMO) and *m*-chloroperbenzoic acid (*m*-CPBA) were supplied by Alfa Aesar. Other commercially available chemicals were laboratory-grade reagents from local suppliers. Styrene was passed through a pad of neutral alumina before use. Chiral salen ligand and chiral homogeneous catalyst salen Mn(III) were synthesized according to the standard literature procedures [1], and further identified by analysis and comparison of IR spectra with literature [31].

FT-IR spectra were recorded from KBr pellets using a Bruker RFS100/S spectrophotometer (USA) and diffuse reflectance UV–vis spectra of the solid samples were recorded in the spectrophotometer with an integrating sphere using $BaSO_4$ as standard. ^{1}H NMR and ^{31}P NMR were performed on AV-300 NMR instrument at ambient temperature at 300 and 121 MHz, respectively. All of the chemical shifts were reported downfield in ppm relative to the hydrogen and phosphorus resonance of TMS and 85% H_3PO_4, respectively. Number- and weight-average molecular weights (M_n and M_w) and polydispersity (M_w/M_n) were estimated by Waters1515 gel permeation chromatograph (GPC; against polystyrene standards) using THF as an eluent (1.0 mL min^{-1}) at 35 °C. X-ray photoelectron spectrum was recorded on ESCALab250 instrument. TG analyses were performed on a SBTQ600 thermal analyzer (USA) with the heating rate of 20 °C min^{-1} from 25 to 1000 °C under flowing N_2 (100 mL min^{-1}). The Mn contents of the catalysts were determined by a TAS-986G (Pgeneral, China) atomic absorption spectroscopy. SEM were performed on KYKY-EM 3200 (KYKY, China) microscopy. TEM were obtained on a TECNAI10 (PHILIPS, Holland) apparatus. Nitrogen adsorption isotherms were measured at 77 K on a 3H-2000I (Huihaihong, China) volumetric adsorption analyzer with BET method. The conversions (with *n*-nonane as internal standard) and the ee values were analyzed by gas chromatography (GC) with a Shimadzu GC2010 (Japan) instrument equipped using a chiral column (HP19 091G-B213, 30 m × 30 m × 0.32 mm × 0.25 μm) and FID detector, injector 200 °C, detector 30 °C. The column temperature was in the range of 80–150 °C.

2.2. Synthesis of aminomethyl-zirconium poly(styrene-phenylvinylphosphonate)-phosphate (ZAMPS-PVPA)

The synthesis of ZAMPS-PVPA is outlined in Scheme 1.

2.2.1. Synthesis of styrene-phenylvinyl phosphonic acid copolymer (PS-PVPA)

1-Phenylvinyl phosphonic acid (PVPA) was synthesized according to literature [32] and its structures were confirmed by ^{1}H NMR, ^{31}P NMR and FT-IR. ^{1}H NMR ($CDCl_3$): 6.06 (d, 1H), 6.23 (d, 1H), 7.26–7.33 (m, 3H), 7.48 (m, 2H). ^{31}P NMR (CD_3OD): 15.9. IR (KBr): 2710, 2240, 1500, 1200, 1040, 950, 780, 720, 700 cm^{-1}.

1-Phenylvinyl phosphonic acid (3.68 g, 0.02 mol), styrene (18.4 mL, 8 equiv), ethyl acetate (150 mL) and benzoyl peroxide (BPO, 1.04 g, 4.7 mmol) were added in a three-necked round-bottom flask equipped with a reflux condenser, magnetic stirrer, nitrogen inlet and calcium chloride guard tube. The solution was purged with nitrogen for 20 min. The reaction mixture was stirred under nitrogen at 80 °C for 24 h. After cooling down to room temperature, the reaction mixture was washed with distilled water until pH ≈ 6. Then the solution was poured into methanol (300 mL) and the precipitated polymer was collected by filtration and dried in vacuo (7.52 g). ^{31}P NMR (CD_3OD): 36.2. IR (KBr): 3059, 3026, 2925 (CH), 1602, 1493, 1453, 760, 699 (–C_6H_5), 1150 (P=O), 983 (P–O) cm^{-1}. GPC: $M_n = 29560$, $m = 222$, $n = 37$, $M_w/M_n = 2$.

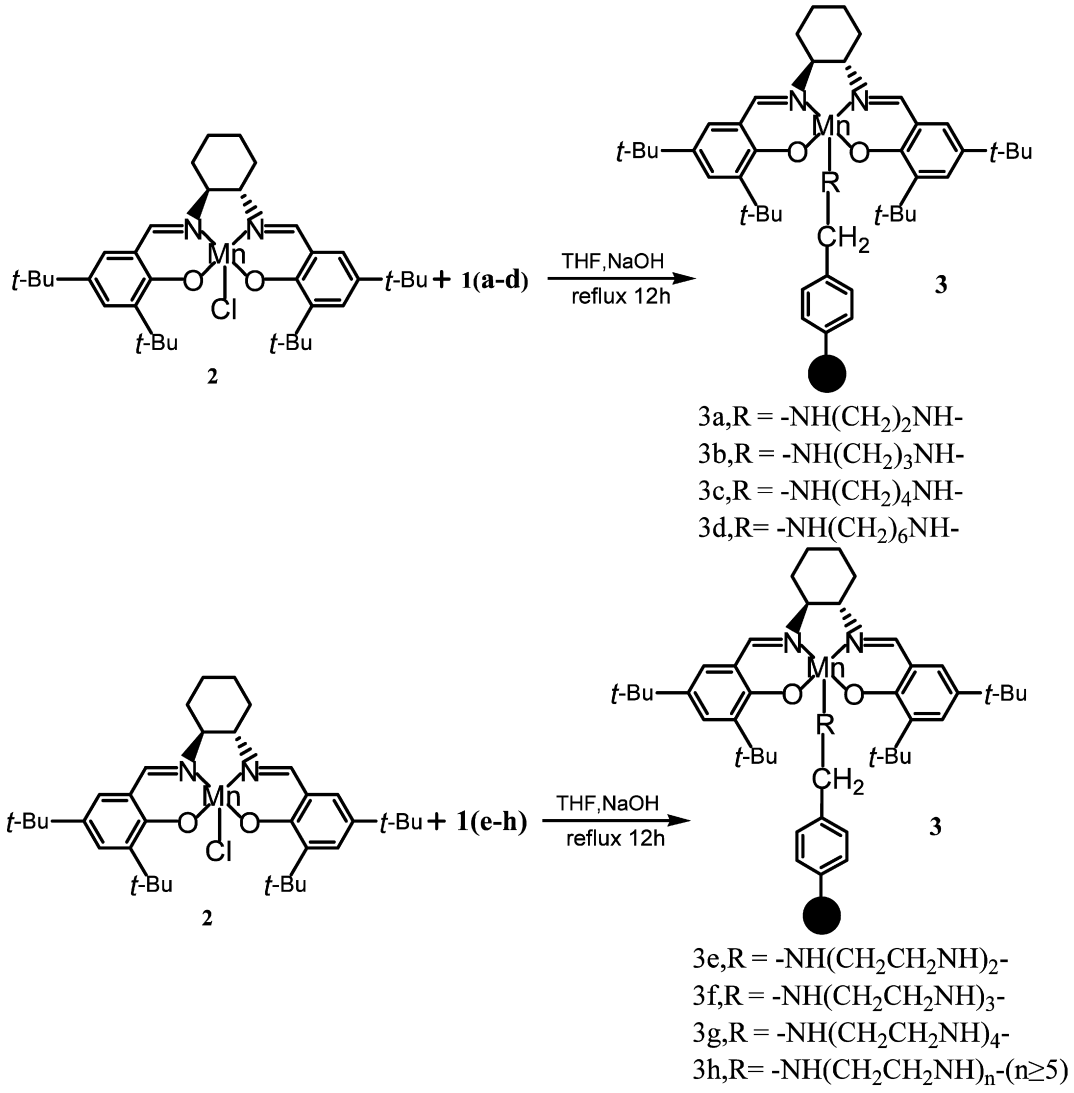

Scheme 2. Synthetic route of the supported catalyst.

2.2.2. Synthesis of zirconium poly(styrene-phenylvinylphosphonate)-phosphate (ZPS-PVPA)

PS-PVPA (5.18 g, 8 mmol) was dissolved in 100 mL THF. In the solution hydrated zirconyl chloride (13.47 g, 24.3 mmol) and hydrated sodium orthophosphate (23.52 g, 16 mmol) aqueous solution were slowly added respectively with vigorously stirring to give white precipitates immediately, then hydrochloride acid (2 mol L^{-1}) was used to adjust the pH in the range of 2–3 and the reaction mixture was kept at 70 °C for 24 h, filtered, washed with deionized water until chloride ion could not be detected and dried in vacuum. White solid of ZPS-PVPA was obtained in 85–90% yields. IR (KBr): 3060, 3026, 2925 (CH), 1632, 1494, 1453, 757, 699 ($-C_6H_5$), 1029 (P=O) cm^{-1}.

2.3. Synthesis of chloromethyl-zirconium poly(styrene-phenylvinylphosphonate)-phosphate (ZCMPS-PVPA)

Chloromethyl methyl ether (9.3 mL), anhydrous zinc chloride (1.92 g, 14.18 mmol) and ZSP-PVPA (6.0 g, 8.55 mmol) were mixed and stirred at 45 °C for 8 h. After cooling, a small amount of water and methanol was added into the mixture, filtered, washed with methanol and acetone and dried in vacuo to obtain zirconium chloromethylated poly(styrene-phenylvinylphosphonate)-phosphate (ZCMPS-PVPA) (7.43 g, 90.3%). IR (KBr): 3026, 2925 (CH), 2337 (O=P–OH), 1605, 1545, 1512, 1495 ($-C_6H_5$), 1271 (P=O), 706 (C–Cl) cm^{-1}.

2.4. Synthesis of aminomethyl-zirconium poly(styrene-phenylvinylphosphonate)-phosphate (ZAMPS-PVPA)

Proper amount of diamines or polyamines (such as a: 1,2-ethylenediamine, b: 1,3-propanediamine, c: 1,4-butanediamine, d: 1,6-hexylenediamime, e: diethylenetriamine, f: triethylenetetramine, g: tetraethylenepentamine, h: polyethylenepolyamine) was mixed with ZCMPS-PVPA (2.63 g), K_2CO_3 (4.5 g, 0.03 mol) and toluene (5 mL) (the molar ratio of amines to chlorine element in ZCMPS-PVPA is 10:1), and the mixture was kept at 80 °C for 12 h. After the reaction, the resinlike product was filtered and washed with substantive amounts of deionized water to remove superfluous amines and dried in vacuo. Reaction yield was always over 90%. The products were abbreviated as 1a, 1b, 1c, 1d, 1e, 1f, 1g and 1h in turn.

2.5. Grafting chiral salen Mn(III) catalyst onto ZAMPS-PVPA

The route for preparing the heterogeneous chiral salen Mn(III) catalysts was outlined in Scheme 2. A solution of chiral salen Mn(III) (4.3 mmol), ZAMPS-PVPA 1a–1h (0.5 g) and adequate

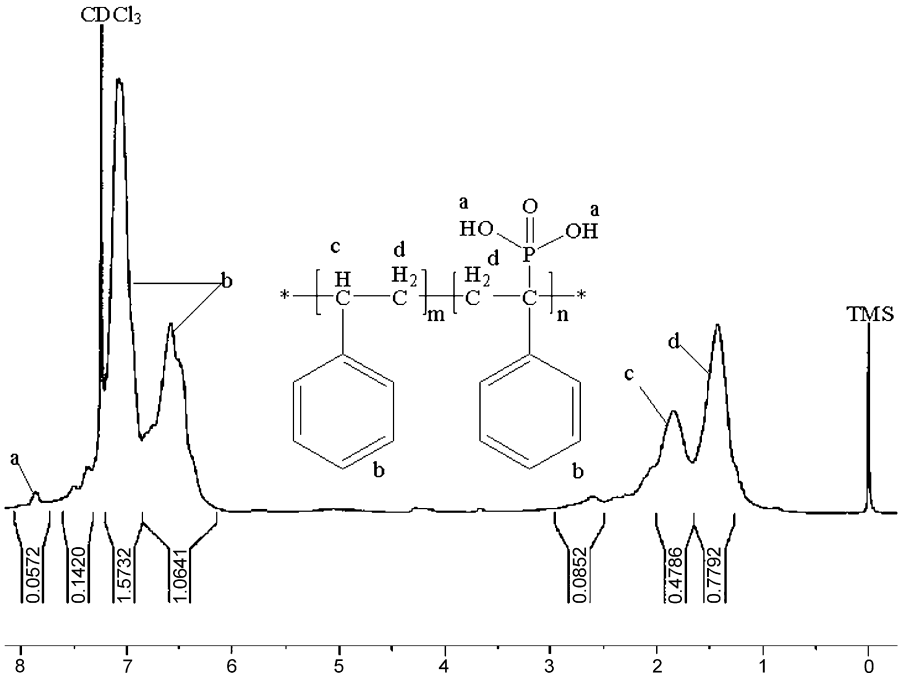

Fig. 1. ^{1}H NMR of copolymer.

amount of sodium hydroxide in tetrahydrofuran (50 mL) was vigorously stirred for 24 h under reflux. The dark brown powder was collected by filtration and washed thoroughly with ethanol, CH_2Cl_2 and deionized water respectively until no Mn could be detected by AAS. The axial coordinate bonding between the supporter and the chiral salen Mn(III) is so strong that chiral salen Mn(III) cannot be eluted from the supporter with water and common organic solvents. The products were abbreviated as ZAMPS-PVPA chiral salen Mn(III) 3a, 3b, 3c, 3d, 3e, 3f, 3g and 3h in turn.

2.6. Asymmetric epoxidation

The activity of the prepared catalysts (3a–3h) were tested for the epoxidation of unfunctionalized olefins in CH_2Cl_2 at −20 °C for 6 h using m-CPBA/NMO as oxidant and with 5 mol% of the catalysts. For NaClO/PPNO system, the reaction was taken out at 20 °C for 24 h and in the presence of 5 mol% of the catalysts. After reaction the organic layer was dried over sodium sulfate, and the catalyst was precipitated out from the solution by adding hexane and kept for subsequent use without further purification. The conversion and ee values of the epoxide were determined by GC.

3. Results and discussion

3.1. The copolymerization reaction of PVPA with styrene

To confirm the structure of copolymer, PVPA and copolymer were investigated by ^{31}P NMR and ^{1}H NMR. The ^{31}P NMR spectra of PVPA showed one peak at 15.9 ppm and the copolymer showed only one peak at 36.2 ppm. Furthermore, there was only one kind of configuration of phosphor atom, which proved the successful copolymerization of PVPA with styrene. The structure of obtained copolymer was also characterized by ^{1}H NMR. A typical ^{1}H NMR spectrum of copolymer is shown in Fig. 1, and the peaks were labeled to assign corresponding protons.

3.2. The chloromethylation reaction of ZPS-PVPA

The chloromethylation reaction of ZPS-PVPA was carried out with chloromethyl methyl ether and anhydrous zinc chloride. Although the chloromethylation reaction of classical polystyrene resin has been carefully studied [33], chloromethylation of ZPS-PVPA has not been reported anywhere. The optimized results were given in Section 2.3, which were obtained by orthogonal design. Under this condition, the chlorine content of the ZCMPS-PVPA is about 13.5%. The strong absorption peak of 706 cm^{-1} in IR spectrum of ZCMPS-PVPA was ascribed to the stretching vibration of C–Cl bond, which indicated that chloromethyl group had been introduced into the benzene ring of ZPS-PVPA.

3.3. Grafting amines on ZCMPS-PVPA

The results of chlorine content analysis revealed that 95–98.96% of chlorine atom in ZCMPS-PVPS had been substituted respectively in preparing 1a–1h. Correspondingly, the sharp C–Cl peak (due to $-CH_2Cl$ groups) at 706 cm^{-1} in the ZCMPS-PVPA practically disappeared or was seen as a weak band after introduction of amines.

3.4. Characterizations of the supports and the heterogeneous chiral catalysts

3.4.1. IR spectroscopy and UV–vis spectroscopy

The synthesized heterogeneous chiral salen Mn(III) catalysts (3a–3h), as well as the neat chiral salen Mn(III) complex were compared with their characterized peaks of IR and UV–vis. As shown in Figs. 2 and 3, the main characteristic bands in the IR spectra of the heterogeneous catalysts (3a–3h) were similar to the neat chiral salen Mn(III) complex 2. All the samples (3a–3h) and complex 2 have shown the same band at 1630 cm^{-1} attributed to the vibration of imine group, which suggest that the heterogeneous catalysts have the similar structure of the neat chiral salen Mn(III) complex 2. Furthermore, an additional band around 3408 cm^{-1} was observed for the samples, which is assigned to the stretching vibration of N–H groups [34]. These observations suggest that the

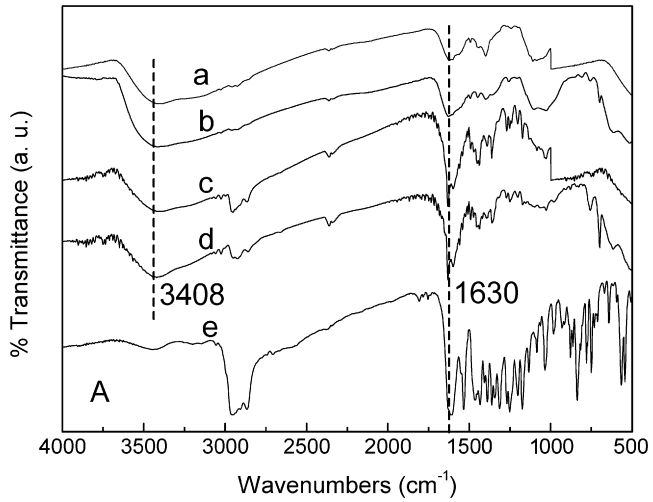

Fig. 2. FT-IR spectra of (a) 3a; (b) 3b; (c) 3c; (d) 3d and (e) the neat chiral salen Mn(III) complex 2.

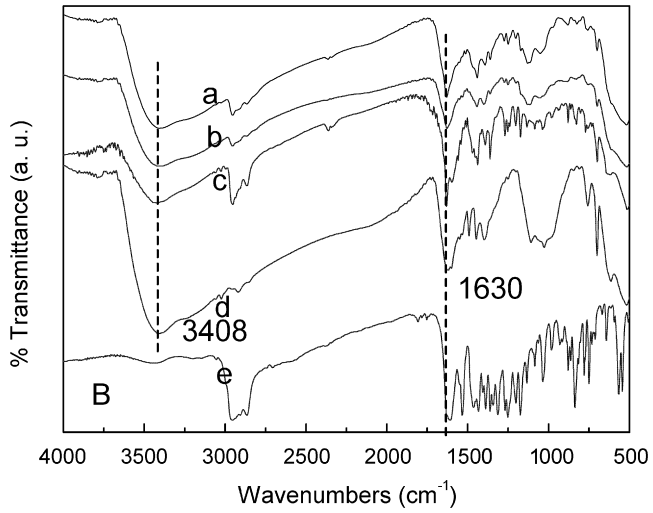

Fig. 3. FT-IR spectra of (a) 3e; (b) 3f; (c) 3g; (d) 3h and (e) the neat chiral salen Mn(III) complex 2.

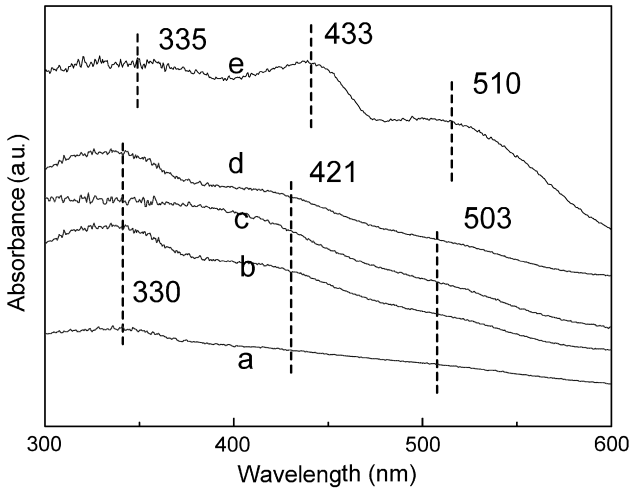

Fig. 4. UV–vis spectra of (a) 3a; (b) 3b; (c) 3c; (d) 3d and (e) the neat chiral salen Mn(III) complex 2.

Table 1
The BET surface area and Mn content of supports and immobilized catalysts.

Supports and immobilized catalysts	BET surface area (m^2/g)	Content of Mn (mmol/g)
1a	89	–
1b	98	–
1c	102	–
1d	112	–
1e	92	–
1f	105	–
1g	115	–
1h	108	–
3a	76	0.63
3b	87	0.65
3c	90	0.66
3d	101	0.68
3e	85	0.77
3f	95	0.82
3g	102	0.89
3h	98	0.92

chiral salen Mn(III) complex has been immobilized onto ZAMPS-PVPA.

The heterogeneous chiral salen Mn(III) catalysts (3a–3d) and the neat chiral salen Mn(III) complex 2 were further confirmed by UV–vis observation (see Fig. 4). The spectra of (3a–3d) have showed features similar to those of complex 2. The bands at 335 nm could be attributed to the charge transfer transition of salen ligand. The band at 433 nm was due to the ligand-to-metal charge transfer transition, and the bands at 510 nm was assigned to the d–d transition of salen Mn(III) complex [35]. On the immobilized salen Mn(III) catalysts, all the characteristic bands appeared in their spectra but the immobilized salen Mn(III) catalysts exhibited a blue shift from 335, 433 and 510 nm to 330, 421 and 503 nm, which indicated that an interaction existed between the salen Mn(III) complex and the diamine or polyamine modified ZPS-PVPA support. The UV–vis spectra of the heterogeneous catalysts (3e–3h) were very similar to the corresponding heterogeneous catalysts (3a–3d).

3.4.2. The BET surface area and Mn content of the supports and immobilized catalysts

Table 1 gives the BET surface area and Mn content of the supports and immobilized catalysts. The manganese contents of the immobilized catalysts (3a–3h) were determined by AAS. Compared with supports (1a–1h), the supported catalysts (3a–3h) exhibited decreased BET surface area, which indicated that chiral salen Mn(III) complex 2 was located mainly on the lamellar of the supporter.

3.4.3. X-ray photoelectron spectroscopy

X-ray photoelectron spectroscopy (XPS) is a powerful technique to investigate the electronic properties of the species formed on the surface. As the electronic environment, e.g. oxidation state and/or spin multiplicity influences the binding energy of the core electrons of the metal. XPS is extensively used to attain detailed information about the state of metal species on the surfaces. Fig. 5 shows the XPS spectra obtained from the neat chiral salen Mn(III) complex and the heterogeneous catalyst 3g. The neat chiral salen Mn(III) complex exhibits Mn $2p_{3/2}$ core level peak at a binding energy of 642.1 eV, while the immobilized salen Mn(III) complex shows a binding energy at 642.3 eV and are in accordance with earlier literature data [36]. The observed increase of chemical shift of 0.2 eV for the immobilized salen complex comparing with the neat complex attributes to the differences in the coordination environment of metal Mn inside the space structure of ZAMPS-PVPA.

3.4.4. Structure analysis of the supports

The possible structure of copolymer is shown in Fig. 6. In the experiment, we want to control the content of PVPA in the copoly-

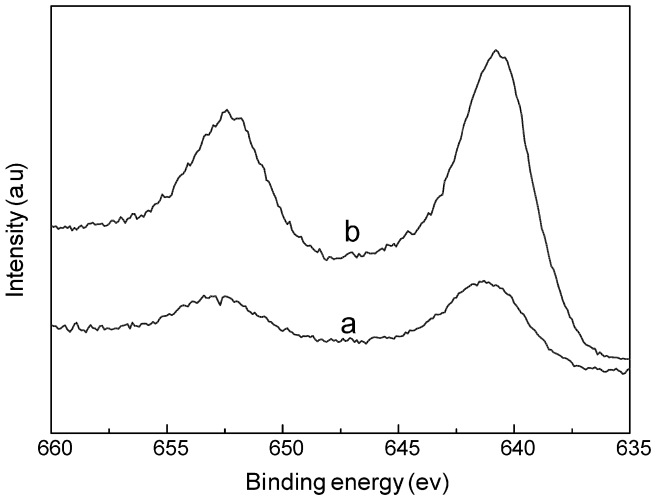

Fig. 5. XPS spectra of (a) the neat chiral salen Mn(III) complex 2 and (b) the heterogeneous catalyst 3g.

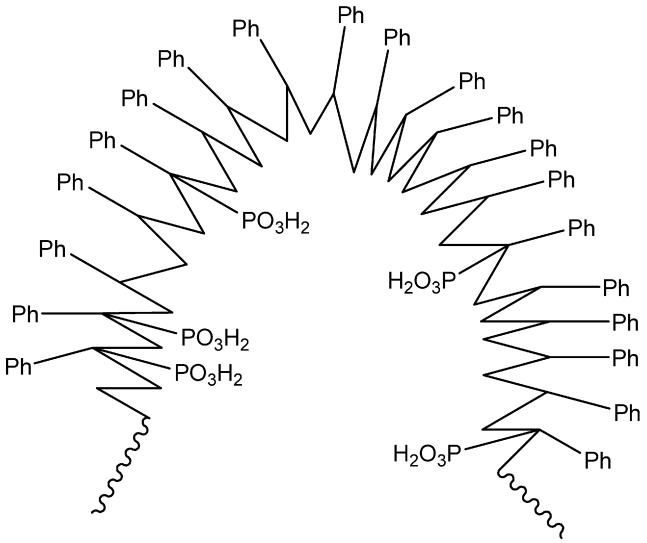

Fig. 6. The possible structure of copolymer.

mer by means of adjusting the amount of initiator and ratio of PVPA to St. Generally speaking, the main segments of the molecule chain are $-(St)_{m_1}-(PVPA)_n-(St)_{m_2}-(PVPA)_n(St)_{m_3}-$ in the copolymer, here the n is usually 1 and seldom more than 2, because the ratio of PVPA to St in the experiment is 1:8 and the content ratio of PVPA to St in the copolymer prepared is in the range of 1:6–9. Therefore, the content of hydrophobic segments of polystyrene is much more than that of hydrophilic segments of PVPA in the copolymer, thus many hydrophilic $-PO_3H_2$ groups might gather together, correspondingly, a great number of hydrophobic segments of polystyrene can form half or part of holes and cavums with different volume and shapes.

The amorphous structure of ZPS-PVPA has been indicated by their XRD, which accounts for its high surface area. It was found by our research group that the hybrid zirconium phosphonate-phosphate has the biggest surface area with the ratio of organic phosphonate to phosphate is 1:2. When aqueous solution of hydrated zirconyl chloride is added, the phosphate, the phosphonic acid in the copolymer and water react with Zr^{4+} immediately to form white colloidal precipitation of ZPS-PVPA. During the process, almost all phosphate in the reaction solution participate in forming the white colloidal precipitation of ZPS-PVPA, while most of organic phosphoric acid in copolymer participate in forming or entering into the white colloidal precipitation and little free phosphoric acid in the copolymer covers on the surface of white colloidal precipitation of ZPS-PVPA. Simultaneously, hydrophobic segments of polystyrene in copolymer which exist half or part of holes and cavums with different volume and shapes are also covered on the surface of the white colloidal precipitation of ZPS-PVPA. The two neighboring $-PO_3H_2$ groups in the copolymer may be in same or in different white colloidal precipitations which will aggregate into bigger colloidal precipitation particles of ZPS-PVPA. Thus, there are probably two kinds of gathering model. Fig. 7a signifies that the two or more neighboring $-PO_3H_2$ groups are in same colloidal precipitation; while Fig. 7b signifies that the two neighboring $-PO_3H_2$ groups are in different colloidal precipitations. In the aggregation process of the colloidal precipitation into bigger particles, many precipitation particles link each other to form even bigger hybrid zirconium phosphonate-phosphate precipitation particles, a great deal of channels, holes and cavums with different volume and shapes are gradually formed. So, if precipitation particles link in the form of model b, different length and shape of channels, holes and cavums will come into being. And if the particles link in the form of model a, the channels, holes and cavums with smaller volume will be formed and cover on the surface of the small precipitation particles.

3.4.5. Analysis of surface morphology

Scanning electron micrograph (SEM) was recorded to understand morphology of the surface of the support and catalyst. The SEM of ZPS-PVPA and the heterogeneous catalyst 3g were shown in Fig. 8, which indicated that the diameter of the particles of the heterogeneous catalyst 3g was in submicron. It was also showed that the catalyst was loose, and various caves, holes, porous and channels with different shape and size were existed in every particles. The TEM photograph of the heterogeneous catalyst 3g was also shown in Fig. 8, which indicated the structure of the heterogeneous catalyst 3g was also loose, its channels, holes and cavums could be discerned clearly, and their sizes were about 20–40 nm. So the catalysts could provide enough space for asymmetric epoxidation of unfunctionalized olefins, which may be one of the main factor of the excellent catalytic activities and properties of the heterogeneous chiral catalysts.

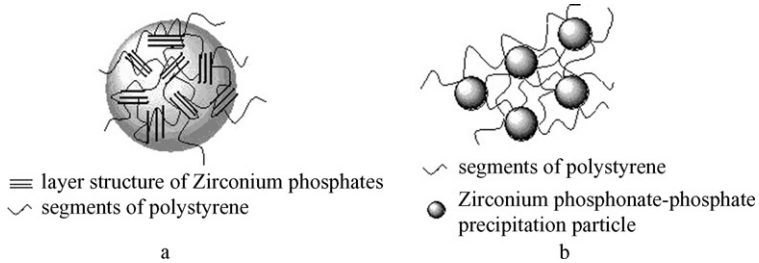

Fig. 7. Two possible gathering model of ZPS-PVPA.

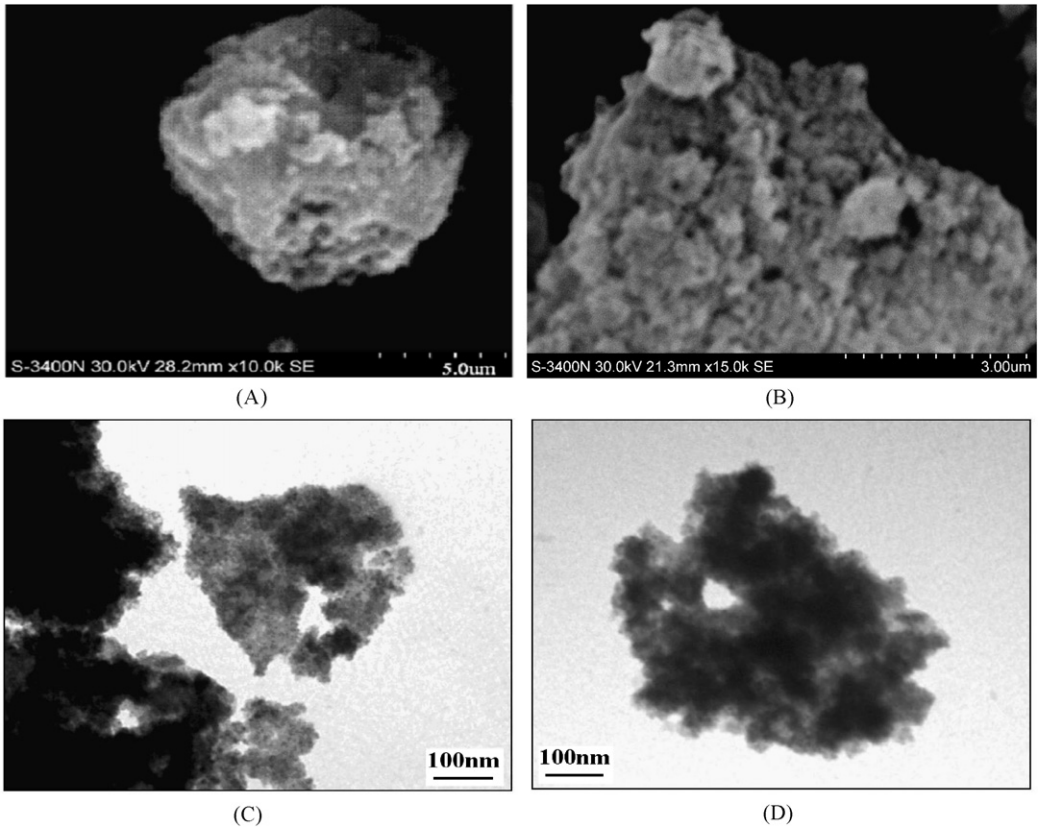

Fig. 8. SEM photograph of (A) ZPS-PVPA, (B) the catalyst 3g and TEM photograph of the catalyst 3g (C and D).

3.5. Enantioselective epoxidation of unfunctionalized olefins

The catalytic activity and selectivity of catalysts (3a–3h) were explored for the asymmetric epoxidation of styrene and α-methylstyrene using m-CPBA/NMO or NaClO/PPNO as an oxidant system. Jacobsen's catalyst 2 was also examined for comparison purposes. The results are summarized in Table 2. All reactions proceeded smoothly, and the heterogeneous catalysts gave high yields of the epoxides and much higher ee values than the homogeneous catalyst under the same conditions. Especially, in the epoxidation of α-methylstyrene, both the conversion and enantiometric excess (ee) could exceed 99% (entry 18). And the increase in ee is mainly attributed to the particular structure of ZPS-PVPA that restrains the free rotation of the intermediate. The similar increase in ee for α-methylstyrene (from 56% to 72%) was also reported earlier for salen Mn(III) complex immobilized on MCM-41 [37]. In the absence of the additive NMO, the activity of 3g apparently decreased, and the enantioselectivity was almost lost for epoxidation of styrene with m-CPBA as an oxidant (entry 10 vs. entry 8). In the NaClO aqueous/organic biphasic system without additive PPNO, it took 24 h for the catalyst 3g to epoxidize α-methylstyrene, and the ee value obtained (60%) was relatively low (entry 20 vs. entry 18), indicating that PPNO as an axial ligand has a pronounced effect on both the activity and the enantioselectivity of the asymmetric epoxidation reaction, which has been reported for other chiral salen Mn(III) catalysts [38–41].

It was also found that the yield and the enantioselectivity increased with increasing linkage lengths of the diamine or polyamine except for polyethylenepolyamine, the similar results were obtained by H.D. Zhang and C. Li [42]. The ee values obtained for the reactions catalyzed by the catalysts (3a–3g) increased from 50% to 72% in asymmetric epoxidation of styrene and from 86% to >99% in asymmetric epoxidation of α-methylstyrene. The results might be due to the immobilized salen Mn(III) complexes which

Table 2
Asymmetric epoxidation of styrene and α-methylstyrene catalyzed by homogeneous and heterogeneous catalysts (3a–3h) with m-CPBA/NMO[a] and NaClO/PPNO[b] as oxidant systems.

Entry	Substrate[c]	Catalyst	Oxidant system	Time	Conv. (%)	ee[d]	TOF[e] $\times 10^{-4}$ (s^{-1})
1	A	2	m-CPBA/NMO	6	98	47	9.07
2		3a	m-CPBA/NMO	6	81	50	7.50
3		3b	m-CPBA/NMO	6	87	55	8.06
4		3c	m-CPBA/NMO	6	90	56	8.33
5		3d	m-CPBA/NMO	6	97	58	8.98
6		3e	m-CPBA/NMO	6	85	66	7.87
7		3f	m-CPBA/NMO	6	92	69	8.52
8		3g	m-CPBA/NMO	6	98	72	9.07
9		3h	m-CPBA/NMO	6	76	62	7.04
10		3g	m-CPBA	6	53	4	4.91
11	B	2	NaClO/PPNO	24	>99	65	2.31
12		3a	NaClO/PPNO	24	86	88	1.99
13		3b	NaClO/PPNO	24	88	90	2.04
14		3c	NaClO/PPNO	24	92	91	2.13
15		3d	NaClO/PPNO	24	96	96	2.22
16		3e	NaClO/PPNO	24	94	86	2.18
17		3f	NaClO/PPNO	24	97	92	2.25
18		3g	NaClO/PPNO	24	>99	>99	2.31
19		3h	NaClO/PPNO	24	90	88	2.08
20		3g	NaClO	24	60	80	1.20

[a] Reactions were carried out at −20 °C in CH_2Cl_2 (4 mL) with styrene (1 mmol), *n*-nonane (internal standard, 1 mmol), NMO (5 mmol), homogeneous (5 mol%) or heterogeneous salen Mn(III) catalysts (5 mol%) and m-CPBA (2 mmol). The conversion and the ee value were determined by GC with chiral capillary columns HP19 091G-B213, 30 m × 0.32 mm × 0.25 μm.

[b] Reactions were carried out at 20 °C in CH_2Cl_2 (2 mL) with PPNO (0.38 mmol) and NaClO (pH 11.5, 0.55 M, 3.64 mL). Other conditions are the same as aforementioned.

[c] A = styrene, B = α-methylstyrene.

[d] (S)-form.

[e] Turnover frequency (TOF) is calculated by the expression of [product]/[catalyst] × time (s^{-1}).

Table 3
The recycles of catalyst 3g in the asymmetric epoxidation of α-methylstyrene.[a]

Run	Time	Conversion (%)	ee (%)[b]	TOF[c] × 10^{-4} (s^{-1})
1	24	>99	>99	2.31
2	24	99	>99	2.29
3	24	98	>99	2.27
4	24	98	>99	2.27
5	24	96	>99	2.22
6	24	95	99	2.20
7	24	95	98	2.20
8	24	94	97	2.18
9	24	92	93	2.13
10	24	90	91	2.08
11	24	80	85	1.85
12	24	72	83	1.67
13	24	58	65	1.34

[a] Reactions were carried out at 20 °C in CH_2Cl_2 (2 mL) with α-methylstyrene (1 mmol), *n*-nonane (internal standard, 1 mmol), PPNO (0.38 mmol), heterogeneous salen Mn(III) catalysts (5 mol%) and NaClO (pH 11.5, 0.55 M, 3.64 mL). The conversion and the ee value were determined by GC with chiral capillary columns HP19 091G-B213, 30 m × 0.32 mm × 0.25 μm.
[b] (S)-form.
[c] Turnover frequency (TOF) is calculated by the expression of [product]/[catalyst] × time (s^{-1}).

may attack active intermediates of salen Mn(V) more expediently with increasing linkage lengths. Whereas, the heterogeneous catalyst 1h only obtained 62% ee in the asymmetric epoxidation of styrene and 88% ee in α-methylstyrene. The proper reason could be that the catalyst 1h has been loaded so much salen Mn(III) that the property of the catalyst 1h is affected.

3.6. The recycling of the supported chiral salen Mn(III) catalyst

To assess the long-term stability and reusability of the supported chiral salen Mn(III) catalysts, α-methylstyrene was used as a mode substrate, and recycling experiments were carried out with the catalyst 3g. After each experiment, the catalyst was precipitated from the reaction system by adding hexane and subsequently used without further purification. The results of the recovered catalyst 3g after thirteen recycling are listed in Table 3. Obviously, reuse of the catalyst 3g in ten times decreased slightly in both the yield and the enantioselectivity. However, after recycling for ten times, any further attempt to recover the catalyst 3g always gave poor yield and enantioselectivity. As can be seen from Table 3, the significant decrease in both the yield and the enantioselectivity was observed in eleventh, twelfth and thirteenth runs.

The nature of the recovered catalyst has been characterized by UV–vis and FI-IR spectra (Fig. 9). It is observed clearly that the characteristic bands of the catalyst at 421, 503 nm^{-1} and 2954, 2864 and 1630 cm^{-1} disappeared or weaken after recycling ten times. These revealed that the active sites of salen Mn(III) complex and the ZPS-PVPA support under basic reaction conditions were partly destroyed. It may be the reason of the decrease of the activity and the enantioselectivity for the eleventh, twelfth and thirteenth runs. In the goal to gain a better understanding of this unique catalytic system, the catalyst 3g was selected as the typical catalyst to investigate the effects of various solvents and reaction temperatures on the enantioselective epoxidation of styrene.

Table 4
The results of the asymmetric epoxidation of styrene catalyzed by the catalyst 3g in different solvents.[a]

Solvent	Time	Conversion (%)	ee (%)[b]	TOF[c] × 10^{-4} (s^{-1})
n-Hexane	6	55	43	5.09
Dichloromethane	6	98	72	9.07
Ethyl acetate	6	92	65	8.52
Acetone	6	92	62	8.52
Acetonitrile	6	95	40	8.80

[a] Reactions were carried out in −20 °C CH_2Cl_2 (4 mL) with styrene (1 mmol), *n*-nonane (internal standard, 1 mmol), m-CPBA (2 mmol), heterogeneous salen Mn(III) catalysts (5 mol%) and NMO (5 mmol). The conversion and the ee value were determined by GC with chiral capillary columns HP19 091G-B213, 30 m × 0.32 mm × 0.25 μm.
[b] Same as in Table 3.
[c] Same as in Table 3.

3.7. Effect of solvent

Table 4 summarizes the results of a comparative study of the enantioselective epoxidation of styrene over the catalyst 3g in various solvents. It was found that dichloromethane was the optimal solvent for the reaction, whereas hexane appeared to be unsuitable for the enantioselective epoxidation of styrene presented here. The difference among these solvents should be that the catalyst 3g is more readily dissolvable in dichloromethane than in hexane. The enantioselectivity was lower in ethyl acetate and acetone than in dichloromethane. In particular, the ee of only 40% was obtained in acetonitrile, possibly indicating that the solvent containing oxygen or nitrogen atoms with a lone electron pair can induce coordination with the metal center of the chiral salen Mn(III) complex, suppressing formation of the active oxygen transfer species (Mn(V)–oxo) in the epoxidation of styrene [43]. Therefore, dichloromethane is considered as a suitable solvent for the enantioselective epoxidation of styrene.

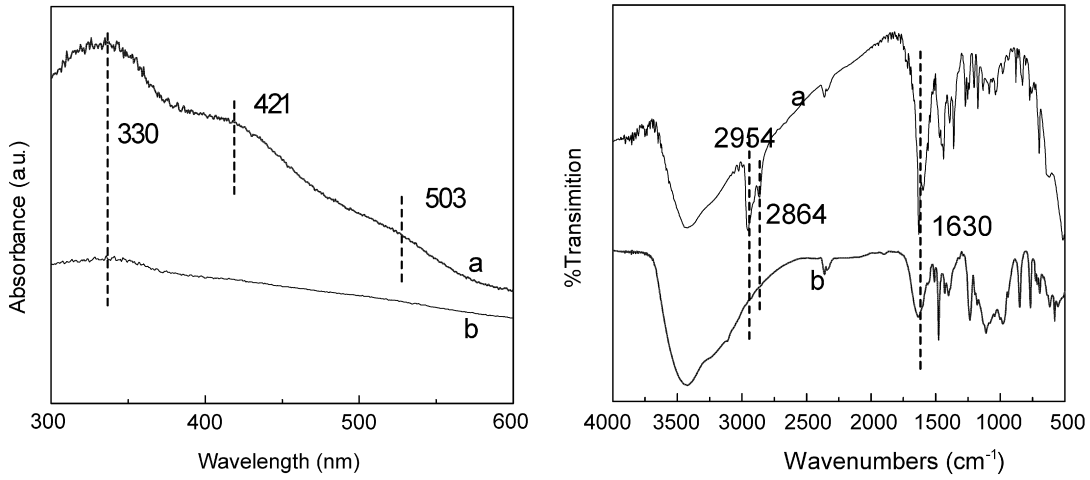

Fig. 9. UV–vis and FT-IR spectra of (a) the fresh catalyst 3a and (b) the used catalyst 3a for ten times.

Table 5
The results of the asymmetric epoxidation of styrene catalyzed by the catalyst 3g in different temperatures.[a]

Temperature (°C)	Time	Conversion (%)	ee (%)[b]	TOF[c] × 10^{-4} (s^{-1})
20	6	85	52	7.87
0	6	86	67	7.96
−20	6	98	72	9.07
−40	6	93	74	8.61
−78	6	90	78	8.33

[a] Same as in Table 4.
[b] Same as in Table 3.
[c] Same as in Table 3.

3.8. Effect of reaction temperature

Table 5 summarizes the catalytic performance of the catalyst 3g at different reaction temperatures. A decrease of reaction temperature from 20 to −20 °C led to the increase of the epoxide conversion from 85 to 98%. However, an increase of enantioselectivity without the change of the yield of epoxide was observed with further decreasing reaction temperature from −20 to −78 °C, which was similar to the results reported previously in Ref. [44]. The reason should be due to both an increase in enantiofacial selectivity in the initial C–O bond forming step and suppression of the trans-pathway in the second step at low temperature [45]. It was encouraging that an enantioselectivity as high as 78% could be obtained when the reaction performed at −78 °C. For asymmetric epoxidation of styrene, the highest ee values of Jacobsen's homogeneous catalysts 2 was 86% reported by Jacobsen's group [44], but the ee values of homogeneous catalysts 2 were 42–62% and the ee values of heterogeneous catalysts were 32–72% as reported by other groups using m-CPBA as oxidant [30,46–48], the difference of the ee values between Jacobsen's group and the others may be attributed to the different reaction processing, for the same reason of this work, so ZAMPS-PVPA chiral salen Mn(III) can gave comparable ee values.

4. Conclusions

In this work, new type of ZAMPS-PVPA-immobilized chiral salen Mn(III) complexes were synthesized and used as catalysts in the asymmetric epoxidation of unfunctionalized olefins. The characterization of FT-IR, UV–vis spectra, AAS, XPS, SEM and TEM for the immobilized chiral salen Mn(III) catalysts indicated that the chiral salen Mn(III) complexes had been successful bonded onto ZAMPS-PVPA. Comparing with the corresponding homogeneous catalyst and other heterogeneous catalysts known from the correlative literatures, the new heterogeneous catalysts showed the comparable or even higher conversions and enantioselectivities, which was mainly attributed to the spatial constraint effects of the special structure of ZPS-PVPA. Moreover, the immobilized catalysts could be conveniently separated from the reaction system through hexane extraction and could be reused at least ten times without significant loss of activity and enantioselectivity. These observations suggested that the new type of ZAMPS-PVPA chiral salen Mn(III) heterogeneous catalysts presented here are promising heterogeneous chiral catalysts for the enantioselective epoxidation of unfunctionalized olefins.

Acknowledgment

Authors are grateful to Southwest University of China for financial support.

References

[1] W. Zhang, J.L. Loebach, S.R. Wilson, E.N. Jacobson, J. Am. Chem. Soc. 112 (1990) 2801.
[2] R. Irie, Y. Ito, T. Katsuki, Synlett. 18 (1991) 265.
[3] M. Palucki, P.J. Pospisil, W. Zhang, E.N. Jacobson, J. Am. Chem. Soc. 116 (1994) 9333.
[4] C.E. Song, S. Lee, Chem. Rev. 102 (2002) 3495.
[5] Y. Zhang, D. Yin, Z. Fu, C. Li, D. Yin, Chin. J. Catal. 24 (2003) 942.
[6] H. Zhang, S. Xiang, J. Xiao, C. Li, J. Mol. Catal. A Chem. 238 (2005) 175.
[7] A.R. Silva, V. Budarin, J.H. Clark, B. Castro, C. Freire, Carbon 43 (2005) 2096.
[8] M. Cardoso, A.R. Silva, B. Castro, C. Freire, Appl. Catal. A Gen. 285 (2005) 110.
[9] P. Piaggio, P. McMorn, D. Murphy, D. Bathell, P.C.B. Page, F.E. Hancock, C. Sly, O.J. Kerton, G.J. Hutchings, J. Chem. Soc. Perkin Trans. 2 (2000) 2008.
[10] H. Zhang, Y. Zhang, C. Li, Tetrahedron: Asymmetry 16 (2005) 2417.
[11] R.I. Kureshy, N.H. Khan, S.H.R. Abdi, I. Ahmael, S. Singh, R.V. Jasra, J. Catal. 221 (2004) 234.
[12] I.F.J. Vankelecom, D. Tas, R.F. Parton, V.V. Vyver, P.A. Jacobs, Angew. Chem. Int. Ed. 35 (1996) 1346.
[13] H. Zhang, S. Xiang, C. Li, Chem. Commun. 9 (2005) 1209.
[14] Y. Sui, X.K. Fu, X.B. Ma, J.R. Chen, R.Q. Zeng, React. Funct. Polym. 64 (2005) 55.
[15] A. Clearfield, D.S. Thakur, Appl. Catal. 26 (1986) 1.
[16] S. Nakayama, K. Itoh, J. Eur. Ceram. Soc. 23 (2003) 1047.
[17] T.M. Suzuki, S. Kobayashi, D.A. Pacheco Tanaka, M.A. Llosa Tanco, T. Nagase, Y. Onodera, React. Funct. Polym. 58 (2004) 131.
[18] A.A. Marti, J.L. Colon, Inorg. Chem. 42 (2003) 2830.
[19] K.M. Parida, B.B. Sahu, D.P. Das, J. Colloid Interface Sci. 270 (2004) 436.
[20] C.V. Kumar, A. Chaudhari, J. Am. Chem. Soc. 122 (2000) 830.
[21] U. Costantino, M. Nocchetti, R. Vivani, J. Am. Chem. Soc. 124 (2002) 8428.
[22] G. Alberti, M. Casciola, Solid State Ionics 145 (2001) 3.
[23] I.O. Benftez, B. Bujoli, L.J. Camus, C.M. Lee, F. Odobel, D.R. Talham, J. Am. Chem. Soc. 124 (2002) 4363.
[24] I.C. Marcu, I. Sandulescu, J.M.M. Millet, Appl. Catal. 227 (2002) 309.
[25] M. Curini, F. Montanari, O. Rosati, E. Lioy, R. Margarita, Tetrahedron Lett. 44 (2003) 3923.
[26] Y. Sui, X.K. Fu, X.B. Ma, J.R. Chen, R.Q. Zeng, React. Funct. Polym. 64 (2005) 55.
[27] Y. Sui, X.K. Fu, R.Q. Zeng, X.B. Ma, J. Mol. Catal. A 217 (2004) 133.
[28] Y. Sui, X.K. Fu, J.R. Chen, X.B. Ma, R.Q. Zeng, Mater. Lett. 59 (2005) 2115.
[29] Y. Sui, X.N. Fang, R.H. Hu, Y.P. Xu, X.C. Zhou, X.K. Fu, Mater. Lett. 61 (2007) 1354.
[30] R.F. Bai, X.K. Fu, H.B. Bao, W.S. Ren, Catal. Commun. 9 (2008) 1588.
[31] M. Palncki, P.J. Pospisil, W. Zhang, E.N. Jacobsen, J. Am. Chem. Soc. 116 (1994) 9333.
[32] B.W. Gong, X.K. Fu, H.S. Shen, L.H. Ma, Y.J. Xia, Fine Chem. 25 (2008) 603.
[33] R.P. Pinell, G.D. Khune, N.A. Khatri, S.L. Manatt, Tetrahedron Lett. 25 (1984) 3511.
[34] K.M. Su, T.Y. Pan, Y.L. Zhang, The Analytic Method of Spectrum, East China University of Science & Technology Press, Shanghai, 2002, p. 100.
[35] L. Lou, K. Yu, F. Ding, X. Peng, M. Dong, C. Zhang, S. Liu, J. Catal. 249 (2007) 102.
[36] A.R. Silva, J.L. Figueiredo, C. Freire, B.D. Castro, Micropor. Mesopor. Mater. 68 (2004) 83.
[37] X.-G. Zhou, X.-Q. Yu, J.-S. Haung, S.-G. Li, L.-S. Li, C.-M. Che, J. Chem. Soc. Chem. Commun. (1999) 1789.
[38] T. Katsuki, Curr. Org. Chem. 5 (2001) 663.
[39] E.N. Jaacobsen, J. Li, Y. Furukawa, L.E. Martinez, Tetrahedron 50 (1994) 4323.
[40] H.D. Zhang, Y.M. Zhang, C. Li, Tetrahedron: Asymmetry 16 (2005) 2417.
[41] H.D. Zhang, Y.M. Zhang, C. Li, J. Catal. 238 (2006) 369.
[42] H.D. Zhang, C. Li, Tetrahedron 62 (2006) 6640.
[43] P. Pietikäinen, A. Haikarainen, J. Mol. Catal. A Chem. 180 (2002) 59.
[44] X.Q. Yao, H.L. Chen, W.R. Lv, G.Z. Pan, X.Q. Hu, Z. Zheng, Tetrahedron Lett. 41 (2000) 10267.
[45] W. Zhang, N.H. Lee, E.N. Jacobsen, J. Am. Chem. Soc. 116 (1994) 425.
[46] K. Yu, L.L. Lou, C. Lai, S.J. Wang, F. Ding, S.X. Liu, Catal. Commun. 7 (2006) 1057.
[47] A.R. Silva, K. Wilson, J.H. Clark, C. Freire, Micropor. Mesopor. Mater. 91 (2006) 128.
[48] S.H. Zhao, P.R. Ortiz, B.A. Keys, K.G. Davenport, Tetrahedron Lett. 37 (1996) 2725.